



Mechanism of the self-condensation of GlcNH₂: insights from *in situ* NMR spectroscopy and DFT study

Lingyu Jia^{a,b}, Xingchen Liu^c, Yan Qiao^c, Christian Marcus Pedersen^d, Zhenzhou Zhang^{b,c}, Hui Ge^a, Zhihong Wei^c, Yanyan Chen^c, Xiaodong Wen^c, Xianglin Hou^{a,*}, Yingxiong Wang^{a,*}

^a Shanxi Engineering Research Center of Biorefinery, Institute of Coal Chemistry, Chinese Academy of Sciences, China

^b Graduate University of Chinese Academy of Sciences, Beijing, China

^c State Key Laboratory of Coal Conversion, Institute of Coal Chemistry, Chinese Academy of Sciences, Taiyuan, China

^d Department of Chemistry, University of Copenhagen, Universitetsparken 5, DK-2100 Copenhagen, Denmark

ARTICLE INFO

Article history:

Received 22 June 2016

Received in revised form

21 September 2016

Accepted 25 September 2016

Available online 27 September 2016

Keywords:

in situ NMR

DFT calculations

Reaction mechanism

Chitin biomass

ABSTRACT

A combined experimental and computational study on the imidazolium ionic liquid-promoted conversion of d-Glucosamine (GlcNH₂) to deoxyfructosazine (DOF) and fructosazine (FZ) was performed. The pathways for the formation of DOF and FZ via self-condensation of GlcNH₂ were investigated by *in situ* ¹³C NMR using site-selectively ¹³C-labeled GlcNH₂. The structural characterization of the reactive species by ESI-MS spectrometry combined with NMR analysis of [¹³C-1]GlcNH₂ indicates that the first carbon (C-1) of GlcNH₂ maps onto the corresponding ring carbons of the intermediate, called dihydrofructosazine [2,5-bis(*d*-arabino-tetrahydroxybutyl)dihydropyrazine], which subsequently is converted to the corresponding pyrazine ring carbons of DOF and FZ respectively. The isotopic-labelling experiments disclose that there are two parallel reaction pathways open to the intermediate dihydrofructosazine, when the reaction takes place in DMSO with [C₂C₁Im][OAc] as catalyst. The theoretical results from DFT calculation indicate that the role of the imidazolium based ILs [C₂C₁Im][OAc] can be envisaged as an acid-base dual activation in catalyzing DOF and FZ formation. It turns out that the acidic cation center exerted significant influences on the energy barriers associated with dehydration reaction. In addition, a critical role of counteranion AcO⁻ is to facilitate dehydrogenation process, leading to the formation of hydrogen. A comparison between the two reaction channels, after the formation of intermediate dihydrofructosazine, indicates that both pathways are plausible and that the pathway to DOF is thermodynamically more favorable than that to FZ. The theoretical results are consistent with the experimental observations, and therefore, a detailed and reasonable reaction mechanism was proposed.

© 2016 Elsevier B.V. All rights reserved.

1. Introduction

Biomasses are promising alternatives for the sustainable supply of fuels and valuable chemicals from the viewpoint of green chemistry [1–4]. Chitin biomasses, in particular, are interesting because they form by far the largest natural source of nitrogen (7 wt% of biologically-fixed nitrogen), which has an underestimated but remarkable potential for the production of high value-added chemicals, especially nitrogen-containing compounds [5–10]. However, the design of more efficient catalysts and the fundamental understanding of the reaction pathways of the chemical transformation

of chitin biomass are not well developed yet due to the diversity and complexity of the available biomass causing many possible side reactions [11,12]. One of the key issues is the formation of a variety of unwanted degradation products referred to as “melanoidins” formed through the Maillard reaction (an important nonenzymatic browning reaction in food sciences), resulting in a mixture of strongly colored and soluble polymers with high molecular weight, which have so far eluded detailed structural characterization [13–15]. An understanding of the mechanistic pathways of chitin biomass conversion is therefore of fundamental interest for development of this field in order to find more efficient catalysts and to prevent undesired reactions.

D-Glucosamine (GlcNH₂), as the building monomer unit of the polysaccharide chitosan, holds the potential to revolutionize the production of value-added nitrogen containing chemicals [16,17].

* Corresponding authors.

E-mail addresses: houxl@sxicc.ac.cn (X. Hou), wangyx@sxicc.ac.cn (Y. Wang).

Efforts to design more efficient catalysts and to get insights into the reaction mechanisms of basic chemical transformations of amino-sugars have been made [5–10]. Currently, the main focus has been on the conversion of GlcNH₂ into deoxyfructosazine (DOF) and fructosazine (FZ), due to their versatile applications, such as flavoring agents in food industry and immunomodulators with potentially pharmacological action and physiological effects [9,18–24]. Nitrogen-containing organic compounds such as pyrazines have a huge market. Typically, the reagent price of DOF and FZ is around \$70/mg and \$32/mg by Santa Cruz Biotechnology, respectively [25]. These compounds are used widely in the pharmaceutical industry, such as integral to best-selling drugs [10]. Therefore, the selective conversion of GlcNH₂ to DOF or FZ is regarded as an important route for the conversion of chitin biomass into high-value added organic chemicals.

The formation mechanisms of DOF and FZ have been investigated [19,21,23,26]. The commonly accepted reaction mechanism is the chain-opening pathway involving the self-condensation of GlcNH₂ in a neutral or weakly acidic aqueous environment [20,21]. In general, the reaction pathways for the production of DOF and FZ from monosaccharides typically involve isomerization, condensation, and dehydration steps [24,26]. Although many different intermediates have already been proposed, it is still difficult to predict whether these intermediates are indeed involved in the product-forming step or merely serve as a reservoir for side products, such as contribution to Maillard browning [13,20]. Thus, knowledge of reactive intermediates or the transition states are crucial for the development of novel catalysts with high product specificity and selectivity for the effective transformation of chitin biomass minimizing side reactions. Reactions show advantages when they are carried out in ionic liquids, either with regard to enhanced reaction rates or improved selectivity [9,24,27–30]. Unfortunately, the experimental and theoretical data to support the mechanistic routes is still lacking and a consensus on the real mechanism at a molecular level has not yet been reached. In particular, GlcNH₂ degradation in the presence of ionic liquid [C₂C₁Im][OAc] catalyst remains less well-understood mechanistically. It is unclear how the nature of [C₂C₁Im][OAc] can affect the chemical reactions [28]. Besides that, relatively little is known about the DOF and FZ distribution in connection with the GlcNH₂ conversion due to the multiple reaction pathways observed [24,26]. Comprehensive understanding of the mechanistic processes leading to DOF and FZ formation via the condensation of GlcNH₂, is crucial for further development to optimize the yield and selectivity of the desired products and thus to improve chitin biomass conversion. In other words, the conceptual design of a biomass process cannot be achieved without knowing details of the reaction path that takes reagents to products [31,32].

Herein, a detailed investigation of the mechanism for the self-condensation of GlcNH₂ with [C₂C₁Im][OAc] as the homogeneous catalyst using *in situ* NMR spectroscopy and quantum chemical studies has been reported. *In situ* ¹³C NMR spectroscopy in combination with a site-selective labelling technique enables us to noninvasively identify and quantify the mixtures of the carbohydrate isomers, the intermediates, and the final products. Our isotopic-labelling experiments disclose that there are two competing reaction pathways for the intermediate, dihydrofructosazine, when the reaction takes place in DMSO with [C₂C₁Im][OAc] as the catalyst. DFT was further employed to investigate the mechanism at the atomic level. The theoretical results highlighted the importance of not only the imidazolium based cationic moiety for “acid activation” of the substrate but also “base activation” of the counteranion of the Ac⁻, which exerted significant influences on the energy barriers associated with dehydration and dehydrogenation process. Based on spectroscopic results in combination with related computational conclusions, a detailed reaction mechanism was therefore

proposed. Consequently, knowledge of reactive intermediates and the reaction mechanism will pave the way for selective transformation of non-edible chitin biomass into high value chemicals with potential industrial applications [9].

2. Experimental section

2.1. Materials

[¹³C-1]GlcNH₂ (99 at.%) was purchased from Qingdao Teng long Microwave Technology Co. Ltd. Detailed information on all other chemicals were described in previous work [9,24].

2.2. Characterization

Liquid phase ¹³C and ¹H nuclear magnetic resonance (NMR) spectra were obtained with a Bruker AV-III 400 spectrometer (9.39T) equipped with auto sampler (400.13 MHz for ¹H, 100.61 MHz for ¹³C) [9,24]. *In situ* ¹³C NMR experiments were performed at 333 K. The reaction mixtures were further qualitatively identified by the positive-ion ESI mass spectrum on a Bruker MicrOTOF-Q III.

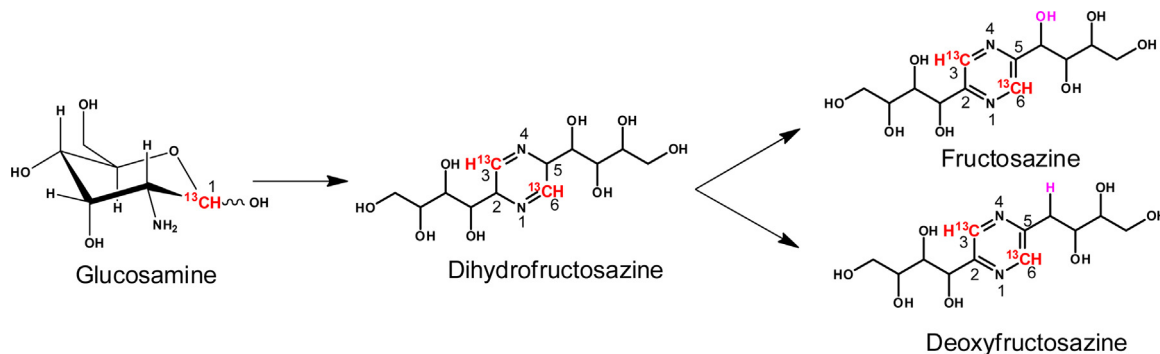
2.3. Procedures for *in situ* NMR studies

A solution of [¹³C-1] GlcNH₂ (4 mg) and 4 mg of the [C₂C₁Im][OAc] in 0.2 ml of DMSO-*d*₆ was prepared in a 5-mm heavy wall NMR tube. The solution was allowed to remain at room temperature for equilibrium. The experimental procedure for [¹³C-1] GlcNH₂ was the same as described for unlabeled GlcNH₂ [9].

2.4. Computational methods

The full geometry optimization of intermediates, products, and transition states (TS) were determined by performing calculations with density functional theory (DFT) theory in combination with the gradient-corrected correlation functional of Lee, Yang, and Parr (B3LYP) with the help of the Gaussian 09 program package [33–37]. The standard basis set 6-311+G(d,p) was applied for all other atoms, which was a proper choice of a model chemistry for most system, especially for organic molecules, because it can provide accurate geometrical parameters and energies with low computational cost [38–45]. All the calculations were performed in the state of ground. No symmetry operations have been applied for any of the structures calculated. Solvation effects were included on the geometry. In the conductor-like polarizable continuum model (CPCM), the solute molecule is placed into a cavity surrounded by the DMSO solvent considered as a continuum medium [46–48]. Dispersion corrections were computed with a locally modified version of Grimme's dftd3-program. Rational damping to finite values for small interatomic distances according to Becke and Johnson (BJ-damping) has been tested [48–51]. It does not only improve the description of noncovalent interactions, but also of the basic properties and particularly the reaction energies. All energies are reported at 298.15 K. With the same basis set, all the energies of structures were obtained after zero-point energy (ZPE) correction and that of optimizations of all the components [52–54]. The correctness of all the optimized structures was confirmed through frequency analysis, where intermediates and products had no imaginary frequencies, while transition states had exactly one imaginary frequency. Transition states (TS) were located by the OPT=TS method and confirmed by the intrinsic reaction coordinate (IRC) approach, to verify that each transition state was connected with the corresponding reactants and products.

All molecular dynamics simulations were performed with the CHARMM program [55,56]. To be specific, we build a large box



Scheme 1. A proposed schematic mechanism for the formation of DOF and FZ from GlcNH_2 condensation via the intermediate dihydrofructosazine.

of $4\text{ nm} \times 4\text{ nm} \times 4\text{ nm}$ with the reactant embedded in 2130 water molecules, and used the CHARMM general force field to heat up the system to the experimental temperature of 333 K, and equilibrate the system for 0.5 ns to fully allow the surrounding water molecules to interact with the reactant [57,58].

3. Results and discussion

3.1. Pathways for DOF and FZ formation from GlcNH_2

The main focus was the detection of reactive intermediates in order to unravel the reaction mechanism, the reaction of d-[$^{13}\text{C}-1$]- GlcNH_2 where the anomeric carbon site C1 (Scheme 1) is ^{13}C -enriched in order to be selectively monitored effectively. Fig. 1 shows a time progression of the *in situ* ^{13}C NMR spectra for the conversion of labeled GlcNH_2 to DOF and FZ catalyzed by $[\text{C}_2\text{C}_1\text{Im}][\text{OAc}]$ in $\text{DMSO}-d_6$ at 60°C (molar ratio of $\text{GlcNH}_2/[\text{C}_2\text{C}_1\text{Im}][\text{OAc}] = 2:1$). Stacked *in situ* ^{13}C NMR spectra are plotted against the reaction time to show the evolution of the reaction substrate, intermediates, and products as the reaction proceeds. As depicted in Fig. 1, in the early reaction stage (2 min), only the resonances (97.8 ppm and 92.6 ppm) attributed to the β/α isomers of d-[$^{13}\text{C}-1$]- GlcNH_2 are observable [59,60]. The changes of the chemical shifts of C-1(β) and C-1(α) of the [$^{13}\text{C}-1$]- GlcNH_2 compared with unlabeled GlcNH_2 may be due to a ^{13}C isotope effect leading to different degrees of nuclear shielding [61,62]. No discernible carbonyl signal from the open-chain forms of GlcNH_2 was observed, presumably due to their short lifetime under the reaction conditions [63]. No conversion of GlcNH_2 except for the isomers is observed after 2 min at 60°C . However, after 17 min of reaction time, more peaks are clearly visible. Notably, a new resonance at 159.2 ppm was clearly observed, which may be attributed to the intermediate, dihydrofructosazine, [2,5-bis(d-arabino-tetrahydroxybutyl)dihydropyrazine], formed by intermolecular nucleophilic cyclization of GlcNH_2 via a dehydration process [21,24,26]. This further suggests that the resonance mentioned above is from an intermediate, as it is formed at an early stage in the reaction and then consumed.

Moreover, in order to get a deeper insight and assign the peaks according to possible intermediates, 2D ^1H - ^{13}C heteronuclear single quantum coherence (HSQC) were exploited to reveal the correlations between proton–carbon (depicted in Fig. S1). Notably, a strong correlation between 159.2 ppm and 7.6 ppm was observed in the HSQC spectrum due to the unsaturated ring carbons and protons of intermediate dihydrofructosazine (depicted by red arrow in Supporting information). Longer reaction time (17–170 min) leads to an increase in intensity of the characteristic resonances assigned to the products DOF (142.8 ppm and 143.5 ppm) and FZ (141.9 ppm) and a decrease in intensity of the resonances associated with dihydrofructosazine (159.2 ppm) [9,18,21,24]. This is

further underpinned by the observation of the decrease of GlcNH_2 signals and the simultaneous increase of the products peaks (DOF and FZ) as the reaction time increased. After 5 h, the GlcNH_2 peaks have virtually disappeared and the ^{13}C NMR spectra is dominated by DOF and FZ peaks. The NMR signal at 159.2 ppm is assigned to dihydrofructosazine, which support the existence of dihydrofructosazine as a key intermediate in the conversion of GlcNH_2 to DOF and FZ. Thus, our results indicate that intermediate dihydrofructosazine is a bifurcation point at which GlcNH_2 can follow either the dehydration pathway to DOF or the dehydrogenation pathway to FZ.

On the other hand, when the reaction further proceeds, the peaks assigned to d-[$^{13}\text{C}-1$]- GlcNH_2 (97.8 ppm and 92.6 ppm) and signals (85.3 ppm, 84.5 ppm, 83.2 ppm, 82.9 ppm, 82.7 ppm, and 79.95 ppm) may be attributed to its isomers or dimers, which decrease correspondingly and eventually disappeared. The results with ^{13}C -labeled GlcNH_2 in this investigation offer a great deal of insight into the mechanisms presented in Scheme 1, disclosing that the first carbon (C-1) of [$^{13}\text{C}-1$]- GlcNH_2 maps onto the corresponding ring carbons (C-3 and C-6) of intermediate, dihydrofructosazine, which is converted to the corresponding pyrazine ring carbons (C-3 and C-6) of DOF and FZ. Surprisingly, by employing site-selectivity ^{13}C -labeled GlcNH_2 , no signals of typically small molecule oxygenated species from biomass conversion, such as 5-hydroxymethylfurfural, levulinic acid or formic acid, were observed in the *in situ* ^{13}C NMR spectra under basic $[\text{C}_2\text{C}_1\text{Im}][\text{OAc}]$ conditions. The recorded ^{13}C NMR spectra only showed DOF and FZ signals, indicating that the GlcNH_2 condensation is selective for the DOF and FZ formation relative to conventional oxygenated products [64]. On the other hand, in relatively high field, several peaks (88.5 ppm, 82.0 ppm, and 80.9 ppm) may be attributed to the formation of colored and soluble polymers presumably due to the condensation polymerization of GlcNH_2 , which have so far eluded structural characterization [13–15,20,23,24].

3.2. Mass spectrometry analysis

To further confirm the generation of reactive intermediates, isomers, and dimers in the condensation reaction of GlcNH_2 , positive-ion ESI mass spectra were qualitatively obtained on a Bruker micrOTOF-Q III. As depicted in Fig. 2, a peak at m/z 111 is corresponding to $[\text{M} (\text{C}_2\text{C}_1\text{Im})^+ + \text{H}]^+$ ($\text{C}_{12}\text{H}_{23}\text{N}_2\text{O}_8$). HCl-free GlcNH_2 showed peaks at m/z 180 corresponding to its protonated molecular ion $[\text{M} (\text{d-}\text{GlcNH}_2)^+ + \text{H}]^+$ ($\text{C}_6\text{H}_{14}\text{NO}_5$) and the ions peaks at m/z 162 and 144 corresponding to mono-dehydrated GlcNH_2 $[\text{M} (\text{d-}\text{GlcNH}_2) + \text{H} - \text{H}_2\text{O}]^+$ and di-dehydrated GlcNH_2 $[\text{M} (\text{d-}\text{GlcNH}_2)^+ + \text{H} - 2\text{H}_2\text{O}]^+$, respectively. The m/z 359 corresponding to $[2 \text{M} + \text{H}]^+$, is likely due to N-glycoside formation between two open-chain form of GlcNH_2 molecules, whereas m/z 341 corresponds to $[2 \text{M} + \text{H} - \text{H}_2\text{O}]^+$ [17,26]. Two other peaks at m/z 305 and 321 were

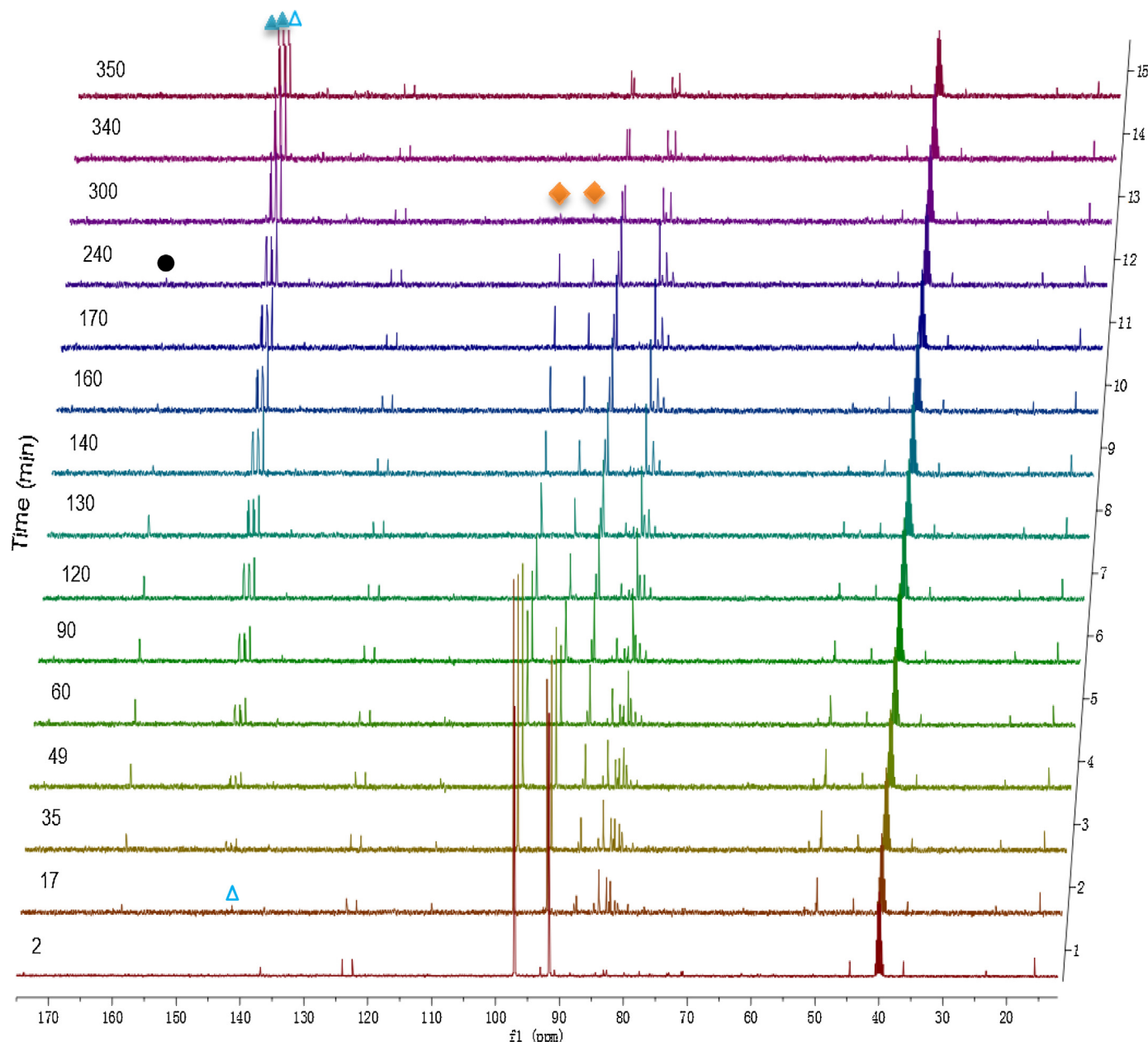


Fig. 1. In situ ^{13}C NMR spectra as a function of reaction time for the condensation of [^{13}C -1]GlcNH₂ catalyzed by 1-ethyl-3-methylimidazolium acetate in DMSO-*d*6 at 60 °C. Notes: ● denotes the peaks of intermediates, ▲ and △ denotes the peaks of DOF and FZ, respectively; ◆ denotes the peaks of the α- and β-anomer of GlcNH₂.

observed. These corresponds to $[\text{M}(\text{DOF})+\text{H}]^+$ and $[\text{M}(\text{FZ})+\text{H}]^+$, which are the main products of the $[\text{C}_2\text{C}_1\text{Im}][\text{OAc}]$ catalyzed reaction [9,18,24]. Notably, a characteristic ion peak at m/z 323 was also clearly observed (indicated by red circle), which was greater than m/z 321 of FZ. The difference in mass spectrum corresponds to two protons and it was believed to be the dihydrofructosazine intermediate [17,26]. The elemental composition of m/z 323 ion, measured by ESI mass spectrum, was $\text{C}_{12}\text{H}_{23}\text{N}_2\text{O}_8$, which agreed with dihydrofructosazine ($\text{C}_{12}\text{H}_{22}\text{N}_2\text{O}_8$) + proton (H). On this basis we draw the conclusion that the intermediate, dihydrofructosazine is formed and this support the *in situ* NMR experimental results.

3.3. Computational results

3.3.1. The analysis of two parallel reaction pathways

On the basis of the time evolution of all the chemical species detected by *in situ* ^{13}C NMR spectroscopy, 6-membered heterocyclic

intermediate, dihydrofructosazine, is formed by a dehydration process via intermolecular nucleophilic addition reactions of two GlcNH₂ molecules. In particular, we were interested in determining the reasonable structure of dihydrofructosazine and also interested in determining how the presence of $[\text{C}_2\text{C}_1\text{Im}][\text{OAc}]$ affected the reaction pathways. Epimerization is a chemical process where a compound is transformed into its diastereomeric counterpart by changing one chiral center, e.g. the epimerization between the sugars N-glucosamine and N-mannosamine, which is catalyzed by a strong base. No epimerization of the C-2 position in GlcNH₂ is expected when catalyzed by $[\text{C}_2\text{C}_1\text{Im}][\text{OAc}]$, which is a weak base. Therefore, only one reasonable structure of dihydrofructosazine existed in the solution, namely, two protons attributed to the chiral center at C-2 and C-5 positions on same sides of the pyrazine ring (A1, Scheme 2a). There are two parallel reaction pathways open to the dihydrofructosazine: FZ is produced via dehydrogenation step while DOF is formed through dehydration and rearrangement pro-

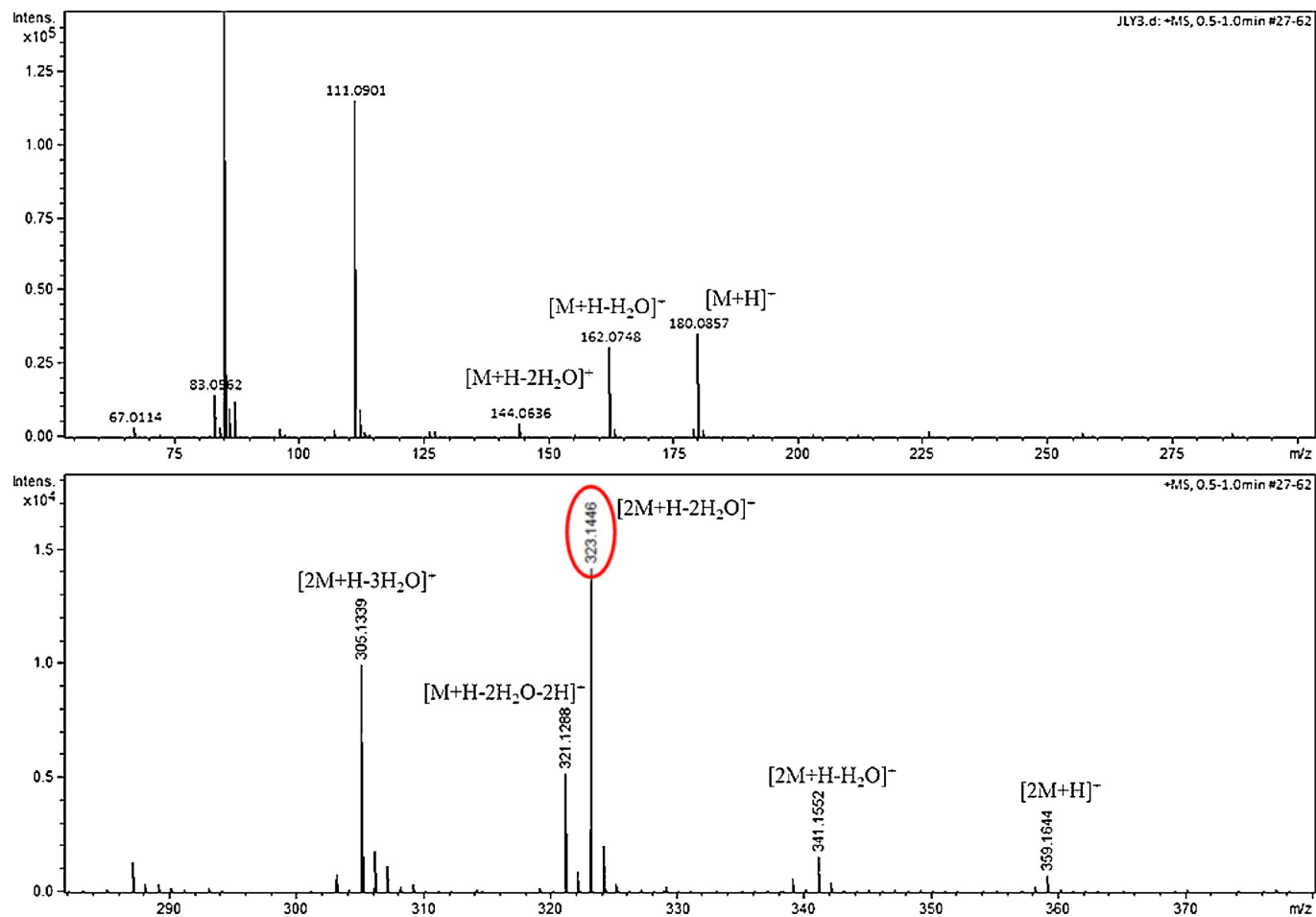


Fig. 2. The positive-ion ESI Mass of an aliquot of sample withdrawn after 20 min during the $[C_2C_1Im][OAc]$ catalyzed reaction.

cess [26]. Detailed DFT calculations were therefore carried out to investigate the competitive reaction channels at atomic level. The optimized structures of all reactants, transition states, and products are depicted in Fig. S2. The hydrogen bonds are indicated by dashed lines.

We initially studied the dehydration reaction process, and three mechanism of dehydration of dihydrofructosazine were investigated. The first path involves an intramolecular proton transfer of neutral dihydrofructosazine (**A1**), where the hydroxyl in the side chain at C-1' position capture a proton from the neighboring pyrazine ring carbon at C-5 position to form a water molecular through a four-centered transition state (**TS1**), it is a high-barrier (49.4 kcal/mol) and moderate exothermic ($\Delta_{\text{react}}G_{298K} = -3.4$ kcal/mol) step [65,66]. Complete detachment of water from this geometry results in formation of a double bond [$R(C=C) = 1.4 \text{ \AA}$] between the adjacent carbon and the carbocation to form an intermediate (**A2**). Subsequent rearrangement reaction of this intermediate to afford DOF (**A3**) is highly exothermic with a reaction free energy of -37.8 kcal/mol (Scheme 2a) [67]. The high barrier is mainly due to the formation of a sterically hindered distorted four-membered transition state, thus, the dehydration reaction may only occur at high temperature and kinetic feasibility under neutral conditions is difficult [65–67].

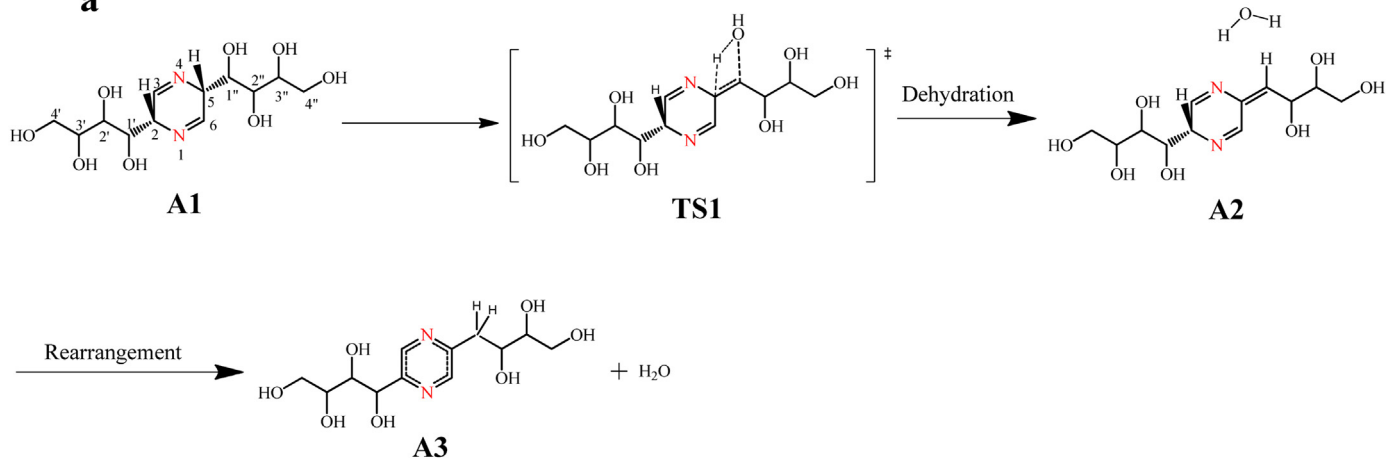
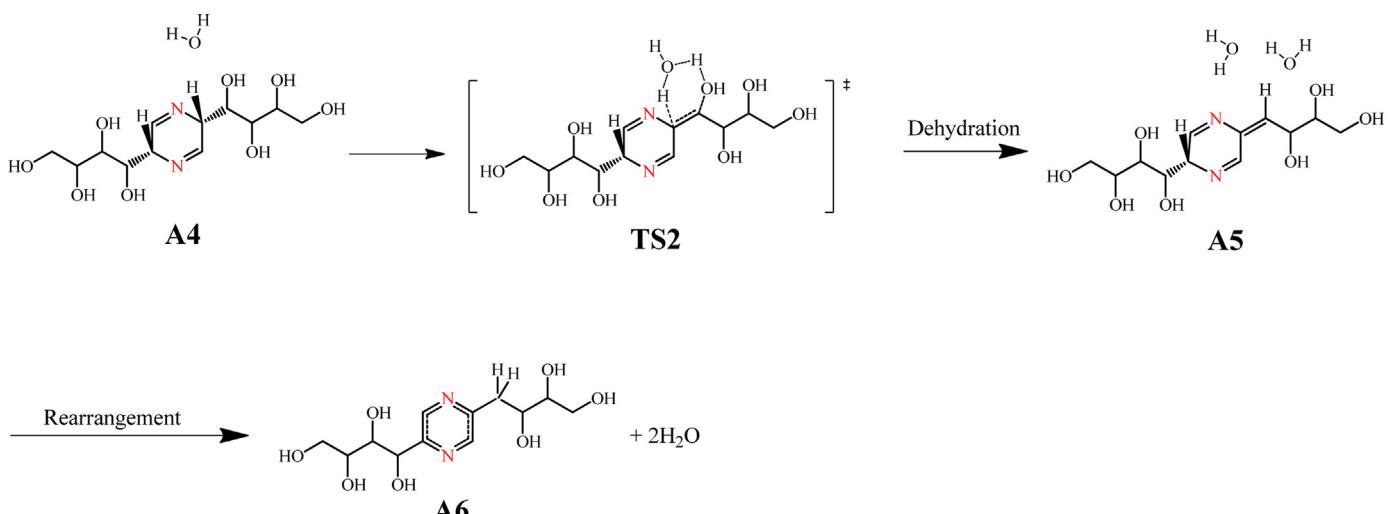
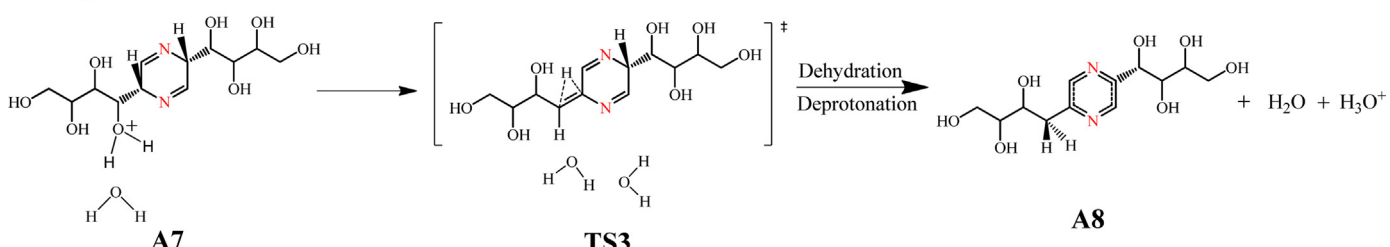
The second path uses a single water molecule to assist dehydration via a six-membered transition state (Scheme 2b) [65]. At higher temperature, water is capable of acting as an acid or base catalyst due to its ionization constant. Inclusion of an explicit water molecule reduces this activation barrier significantly to

39.2 kcal/mol (**A4** \rightarrow **TS2** \rightarrow **A5** \rightarrow **A6**), supporting that this dehydration reaction is a solvent-assisted process [65,68].

To examine the effect of other water molecules in the solvent on the reaction mechanism, we further expand on the choice of water molecule to an explicit water droplet. For this purpose, classical MD simulations were introduced to locate the positions of all the important water molecules that interact closely with the reactant (intermediate, dihydrofructosazine, Fig. S3, detailed information provided in SI) [55,56]. From the equilibrated structure, we then delete all the irrelevant water molecules, and only leave those that are closely interacting with the reactant (depicted by green dashed circle in Fig. S2) and form a droplet of water around the reactant. Apart from building this new model that contains explicit water droplet to account for local solvent effect, we also used the continuum medium model in Gaussian to account for long range solvent effect.

Herein, two dehydration reaction processes through different transition states were investigated. The first involves an intramolecular proton transfer to form water molecular through a four-centered transition state. However, it turns out that the reaction barrier via a four-membered transition state we obtained using the new model (**TS1'**) only has a marginal difference of 1 kcal/mol compared to the previous “four-membered transition state” model (Fig. 3). Thus, the result presented above clearly indicated that all the other surrounding water molecules are not important for this dehydration process.

In Fig. 4, it can be seen that the barrier is lowered by 5 kcal/mol compared to the previous “one-water” model (Scheme 2b). The

a**b****c**

Scheme 2. (a) Schematic representation of dehydration under neutral condition .(b) Schematic representation of dehydration promoted by the inclusion of one explicit water molecule. (c) Schematic representation of dehydration promoted by the acidic media.

results obtained have shown that dehydration is indeed a solvent-assisted process. Besides that, the one water molecule involved in six-membered ring from the solvent plays a decisive role in lowering the barrier. It was demonstrated that the water-free dehydration (four-membered transition state) is impossible under moderate conditions due to large ring strain in TS geometries. Dehydration assisted by water molecules are required to relax the ring strain of the hydrogen-bond network. It is important to notice that although the new model *via* a six-membered transition states lowering energy barrier (TS2'), the obtained product (A5') surrounded by water molecules is thermodynamically unfavorable due to its significant endothermicity (27.91kcal/mol).

Earlier computational studies have shown that the activation barrier for the dehydration of protonated sugars were lowered significantly compared with neat sugars, therefore, we wondered if there is a similar enhancement by protonation for dihydrofructosazine [65–70]. The most acidic proton in the imidazolium cation is H-2 of [C₂C₁Im][OAc], which is therefore expected to activate dihydrofructosazine as an acid catalyst for the dehydration [71,72]. That is to say, the transfer of this proton (H-2) from the cation to the substrate, namely protonation, is facile, thus catalyzing reaction and leading to the desired products [28,71]. Even though all hydroxyl groups of dihydrofructosazine can be protonated in acidic solution, the direct dehydration of dihydrofructosazine to DOF is

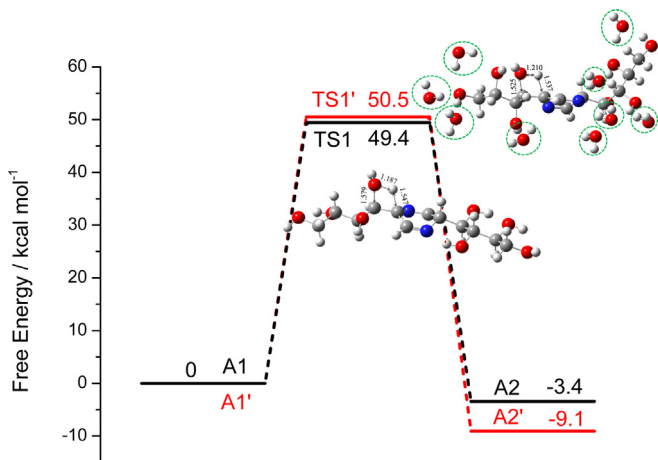


Fig. 3. Potential energy surfaces at 298.15 K for the dehydration reaction pathways via four-membered transition states.

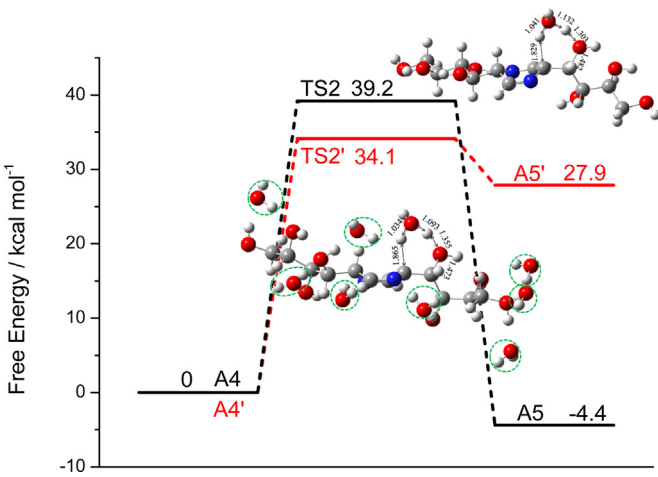


Fig. 4. Potential energy surfaces at 298.15 K for the dehydration reaction pathways via six-membered transition states.

initiated by the protonation of the hydroxyl group on one side chain at C-1' position [56]. This leads to a cascade of reactions which we have studied computationally to get insight into the reaction mechanisms (**Scheme 2c**).

Initially, protonated dihydrofructosazine (**A7**) with one hydroxyl group as the protonation site acts as a good leaving group. Thus, the C—OH₂⁺ bond cleavage occurs *via* the dehydration transition state (**TS3**) facilitated by a rearrangement through hydrogen transfer process (1,2-hydride shift) leading to the formation of product (**A8**). This step presents a barrier of 34.8 kcal/mol, followed by spontaneous deprotonation of the addition product (**Scheme 2c**) [69,70,73]. This barrier is substantially lower than that for neutral dihydrofructosazine (**A1**) dehydration through a four-centered transition state (**TS1**, 49.4 kcal/mol) depicted in **Fig. 5**. The removal of the water appears to be the rate controlling step. This clearly suggests that dihydrofructosazine dehydration is acid-catalyzed at experimental conditions. Furthermore, a new model catalyzed by acidic proton that simultaneously contains explicit water droplet was investigated. Inclusion of explicit water droplet reduces this activation barrier significantly to 30.7 kcal/mol (**A9** → **TS4** → **A10**) compared to pure solvent pathway (**TS2'**), which was depicted in **Fig. 4**. Substantial reduction in this energy barrier, therefore, clearly demonstrate that the acidic H-2 in the imidazolium cation of [C₂C₁Im][OAc] indeed play a key role in promoting the dehydration of dihydrofructosazine. Thus, we see

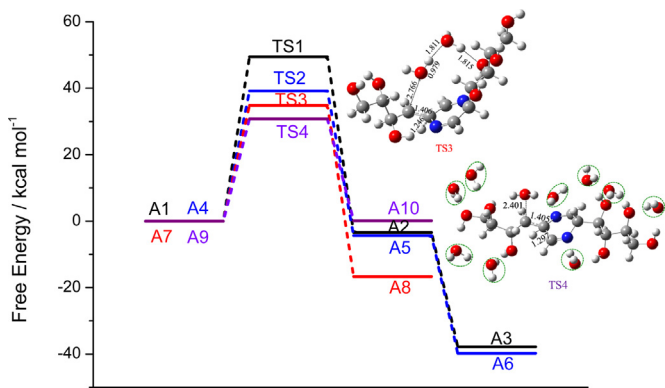
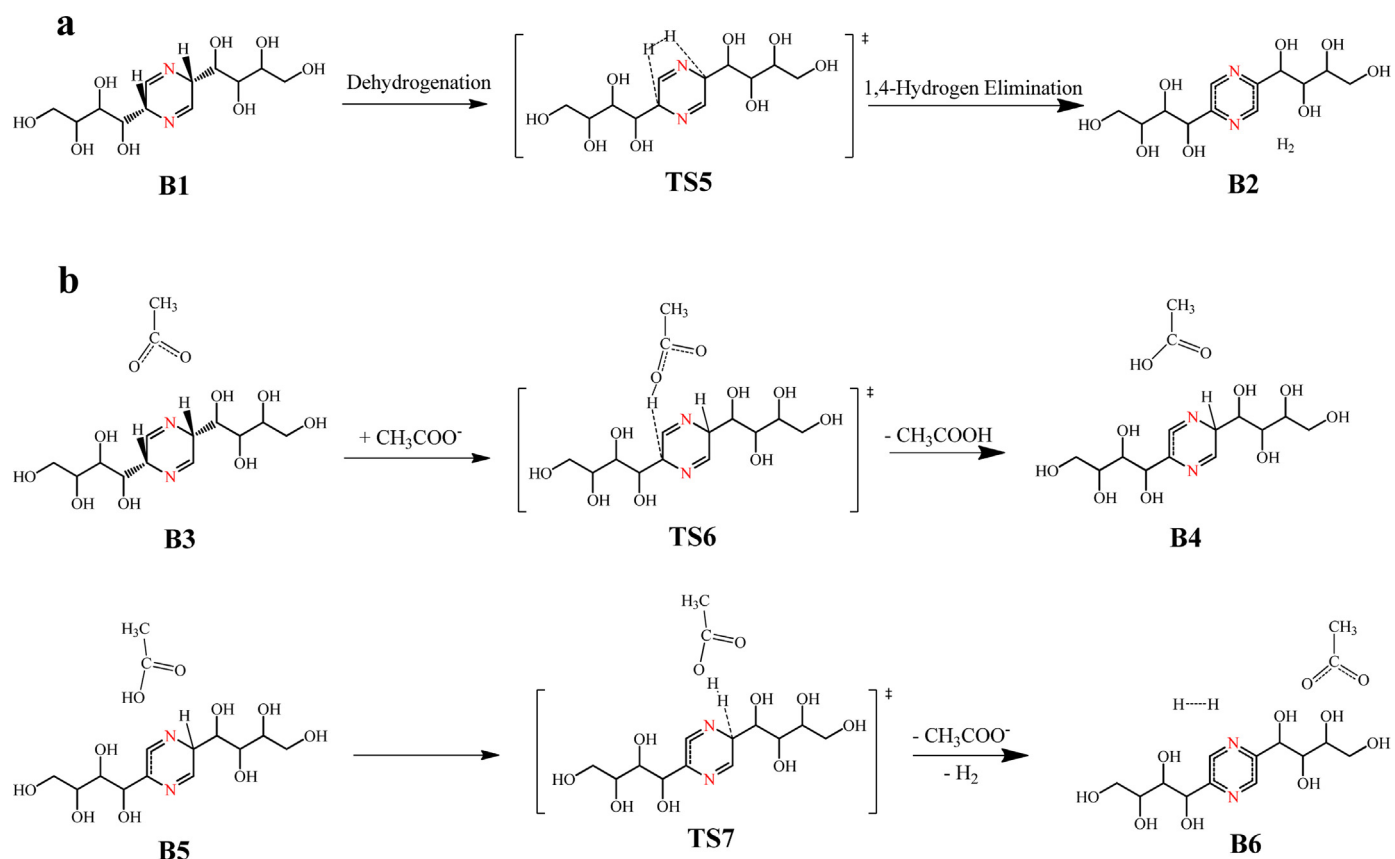


Fig. 5. Potential energy surfaces at 298.15 K for three dehydration reaction pathways. Note: optimized structures of transition states with selected bond lengths in Å for the dehydration processes.

that the highest point along the potential energy surface is the transition state for the dehydration, which has an apparent activation free energy of 30.7 kcal/mol (**Fig. 5**). This value is consistent with the sugar dehydration barrier of 30~35 kcal/mol reported previously and is potentially the rate-determining step [69,70]. This supports the hypothesis that the acidic cation of [C₂C₁Im][OAc] play a key role in lowering the energy barriers.

Dehydrogenation process is another competitive reaction pathway to dihydrofructosazine. Based on the epimerization mechanism, it was found that the transition state for hydride transfer is the *syn*-periplanar conformations occurring on the same side of the dihydrofructosazine with respect to the hydrogen loss [73,74]. Two mechanisms are studied. In the control reaction pathway (**Scheme 3a**), two protons attributed to the chiral centers at C-2 and C-5 positions on same sides of the pyrazine ring firstly approach each other to form a bridge (**TS5**) and then the two hydrogens come off as H₂ simultaneously (**B1** → **TS5** → **B2**). This process is similar to the mechanism of dissociation of 1,4-cyclohexadiene to benzene and H₂ [73]. The pathway for 1,4-hydrogen elimination mentioned above was based on thermochemical calculations alone. It occurs with a relatively free energy barrier of $\Delta G_{298K} = 34.2$ kcal/mol and is moderately exothermic (-6.4 kcal/mol), indicating that this dehydrogenation process is energetically favorable. Previous experimental studies reported that dialkylpyrazine can be obtained from corresponding dihydropyrazine under basic conditions using KOH or NaOH, indicating that base could facilitate dehydrogenation process [75]. Therefore, we wonder whether there is a similar enhancement for dihydrofructosazine when the reaction was catalyzed by [C₂C₁Im][OAc]. With the counteranion AcO⁻ as the basic catalyst it is expected to activate the dihydrofructosazine and thus facilitate the release of hydrogen [71,72]. Insights into the mechanistic pathways, there are two main steps in the whole process (**Scheme 3b**). We propose that the AcO⁻ firstly capture a proton belonging to the chiral center at C-2 position (**B3**) with an energy barrier of 21.7 kcal/mol (**TS6**). The first part of the mechanism was predicted to proceed fast, whereas thermodynamically less favored (**B4**, 22.8 kcal/mol). In the second part, the acetic acid formed provides a proton to combine with hydride belonging to the chiral center at C-5 position (**B5**) and finally hydrogen is formed with an activation free energy of 18.1 kcal/mol (**TS7**). The overall reaction free energy for the dehydrogenation is exothermic by -10.2 kcal/mol (**B6**). This low barrier can be attributed, in part, to the substantial stabilization of the products due to the resonance delocalization of the π system in FZ. It can be concluded that the counteranion AcO⁻ acts exactly as a base catalyst. An inspection of the overall potential energy surfaces shown in **Fig. 6** reveals the apparent activation free energy to FZ through dihydrofructosazine



Scheme 3. (a) Schematic representation of 1,4-H₂ elimination. (b) Schematic representation of 1,4-H₂ elimination promoted by basic media.

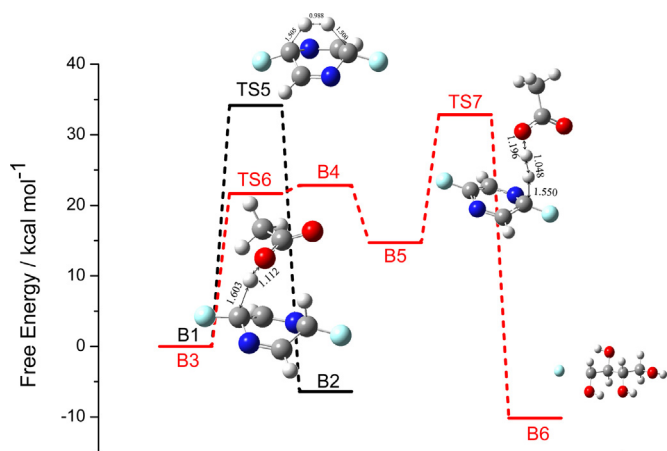


Fig. 6. Potential energy surfaces at 298.15 K for two parallel dehydrogenation reaction pathways. Note: optimized structures of transition states with selected bond lengths in Å for the dehydrogenation processes.

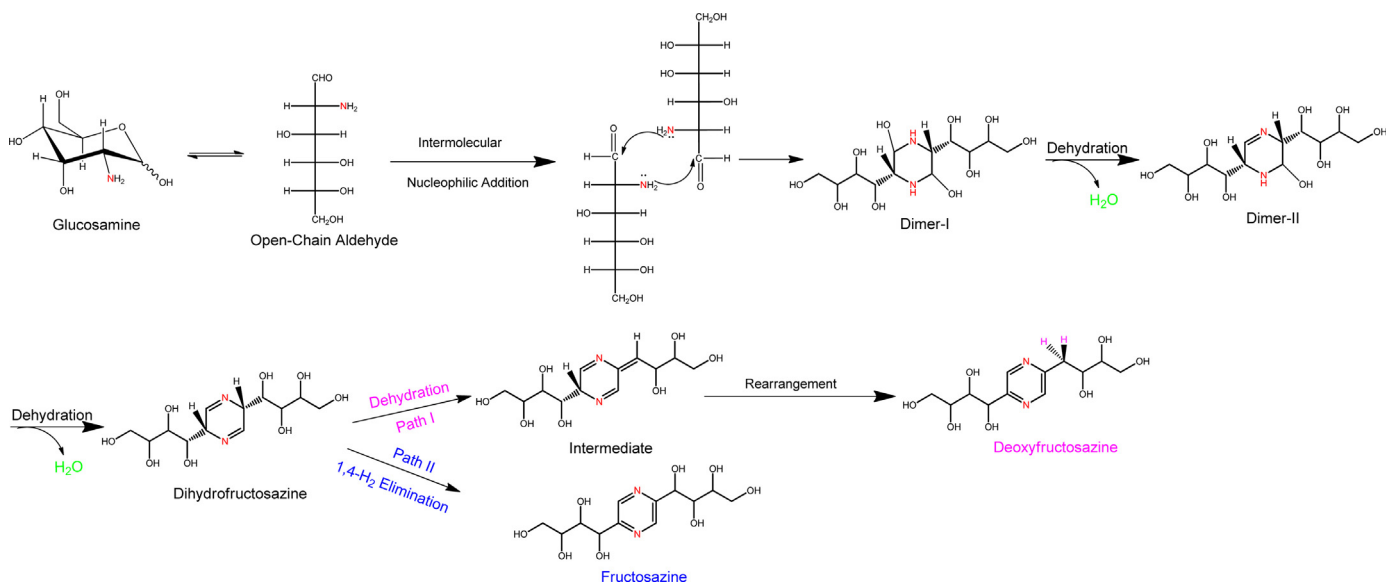
is 32.8 kcal/mol, which is similar to that control reaction pathway (34.2 kcal/mol). Thus, calculations suggest that there are two potentially competitive reaction pathways in the dehydrogenation process.

As discussed above, [C₂C₁Im][OAc] may play a key role in catalyzing the dehydration and dehydrogenation of dihydrofructosazine to DOF and FZ by lowering the energy barriers. The role of the imidazolium based ILs [C₂C₁Im][OAc] has been envisaged as an “acid base dual activation in catalyzing DOF and FZ formation. It turns out that the acidic cationic center exerted significant influences on the energy barriers associated with dehydration reaction, while the role of the counteranion AcO⁻ is to affect proton

and hydride transfer, leading to the formation of hydrogen. A comparison between these two reaction channels, after the formation of intermediate dihydrofructosazine, indicates that both pathways are plausible and that the pathway to DOF is thermodynamically more favorable than that to FZ. The present work provide a molecular level understanding of the mechanism of catalysis by [C₂C₁Im][OAc] and reveal the unique ability of ILs to modulate reactivity and selectivity of organic reactions [71,72]. The mechanism of catalysis highlights the importance of not only the imidazolium based cationic moiety for ‘acid activation’ of the intermediate dihydrofructosazine with the C-2 hydrogen but also ‘base activation’ of the intermediate with the counteranion AcO⁻ of the IL. In addition, hydrogen bonding interactions were also found between the catalyst [C₂C₁Im][OAc] and the substrate, which may stabilize the substrates, transition states and products leading to lower energy barriers. These calculations suggest a plausible explanation for the two parallel reaction pathways of dihydrofructosazine, and the results stated above are in agreement with experimental data.

3.4. Proposed mechanism

By combining the results from the experimental investigations with those obtained computationally, a comprehensive mechanistic picture on the underlying processes of GlcNH₂ conversion is presented in this work (Scheme 4). In the early stage of the reaction, GlcNH₂ mainly showed the α -glycopyranose form in DMSO before reaction, and [C₂C₁Im][OAc] catalyst therein facilitated the mutarotation to produce β -glucopyranose through a ring opening process [31,76]. Dimer-I could then be formed from two acyclic GlcNH₂ molecules by intermolecular nucleophilic attack, which could be confirmed by the ion peak at *m/z* 359 corresponding to [2M+H]⁺ (depicted in Fig. 2). The *m/z* 341 corresponding to Dimer-



Scheme 4. Possible mechanism for the selective formation of DOF and FZ from GlcNH_2 .

II can also be due to N-glycoside formation, followed by losing one water molecule. Furthermore, the 6-membered heterocyclic intermediate, namely, dihydrofructosazine, was formed through loss of one water molecules, which in turn can act as a reservoir for both DOF and FZ [9,24]. Evidence for the formation of dihydrofructosazine has been obtained through mass spectrometric studies (the base ion peak at m/z 323 in positive-ion mode) and *in situ* ^{13}C NMR spectroscopy with characteristic peak at 159.2 ppm. Notably, by combining NMR spectroscopy experiments and density functional theory (DFT) calculations, we can draw the conclusion that the conversion of dihydrofructosazine mainly occurs via two competing pathways, in which DOF is formed *via* loss of one water molecule and a subsequent rearrangement reaction process while FZ was formed simultaneously *via* 1,4-hydrogen elimination. In addition, the dehydrogenation product analysis was conducted using gas chromatography with a thermal conductivity detector. Results indicated that the main gaseous product indeed was hydrogen, which is depicted in Fig. S4. The *in situ* ^{13}C NMR spectroscopy, in combination with computational chemistry and mass spectrometric spectroscopy, therefore, can identify the chemical structure of the intermediates and thereby give insights into the reaction pathways leading to the products.

4. Conclusion

In summary, this work provides a molecular level understanding of the reaction process for the IL-promoted conversion of GlcNH_2 to DOF and FZ, and also a new direction in the search for catalyst systems allowing nitrogen compounds formation from chitin biomasses. *In situ* ^{13}C NMR spectroscopy has been employed to identify reactive intermediates and elucidate the reaction pathways for the $[\text{C}_2\text{C}_1\text{Im}][\text{OAc}]$ catalyzed conversion of GlcNH_2 to DOF and FZ. The structural characterization of the reactive species by ESI-MS spectrometry combined with NMR analysis of $[^{13}\text{C}-1]\text{GlcNH}_2$ reveal that the first carbon (C-1) of GlcNH_2 maps onto the corresponding ring carbons of dihydrofructosazine, which subsequently is converted to the corresponding pyrazine ring carbons of DOF and FZ. Our isotopic-labelling experiments indicate that intermediate dihydrofructosazine is a bifurcation point at which dehydration and dehydrogenation can follow either the pathway to DOF or the pathway to FZ. The theoretical results disclose that the acidic cation center exerted significant influences on the energy

barriers associated with dehydration reaction. In addition, a critical role of counteranion AcO^- is to facilitate dehydrogenation process, leading to the formation of hydrogen. The mechanism of catalysis highlights the importance of not only the imidazolium based cationic moiety for “acid activation” of the intermediate dihydrofructosazine with the C-2 hydrogen but also “base activation” of the dihydrofructosazine with the counteranion of the $[\text{C}_2\text{C}_1\text{Im}][\text{OAc}]$. The quantum chemical results are consistent with the experimental observations, and therefore, a comprehensive and reasonable reaction mechanism has been proposed based on experimental and computational setup.

Acknowledgements

The calculations were supplied by the Tianhe-2 in LvLiang Cloud Computing Center. The authors would like to acknowledge the financial support from the Major State Basic Research Development Program of China (973 Program) (No. 2012CB215305) and Natural Science Foundation of China (No. 21106172, 21403273). Yan Qiao thanks the Chinese Academy of Sciences (2013YC002) and the Youth Innovation Promotion Association of Chinese Academy of Sciences (2011137) for financial support. Christian Marcus Pedersen acknowledges the CAS President's International Fellowship Initiative (2015VMB052).

Appendix A. Supplementary data

Supplementary data associated with this article can be found, in the online version, at <http://dx.doi.org/10.1016/j.apcatb.2016.09.058>.

References

- [1] A. Corma, S. Iborra, A. Velty, Chem. Rev. 107 (2007) 2411–2502.
- [2] M. Yabushita, H. Kobayashi, A. Fukuoka, Appl. Catal. B: Environ. 145 (2014) 1–9.
- [3] H. Li, Z. Fang, J. Luo, S. Yang, Appl. Catal. B: Environ. 200 (2017) 182–191.
- [4] M. Huang, J. Luo, Z. Fang, H. Li, Appl. Catal. B: Environ. 190 (2016) 103–114.
- [5] C.K.S. Pillai, W. Paul, C.P. Sharma, Prog. Polym. Sci. 34 (2009) 641–678.
- [6] X. Chen, S.L. Chew, F.M. Kerton, N. Yan, Green Chem. 16 (2014) 2204–2212.
- [7] M.W. Drover, K.W. Omari, J.N. Murphy, F.M. Kerton, RSC Adv. 2 (2012) 4642–4644.
- [8] K.W. Omari, L. Dodot, F.M. Kerton, ChemSusChem 5 (2012) 1767–1772.
- [9] L. Jia, C.M. Pedersen, Y. Qiao, T. Deng, P. Zuo, W. Ge, Z. Qin, X. Hou, Y. Wang, Phys. Chem. Chem. Phys. 17 (2015) 23173–23182.

- [10] N. Yan, X. Chen, *Nature* 524 (2015) 155–157.
- [11] H. Kimura, M. Nakahara, N. Matubayasi, *J. Phys. Chem. A* 117 (2013) 2102–2113.
- [12] L. Hu, L. Lin, Z. Wu, S. Zhou, S. Liu, *Appl. Catal. B: Environ.* 174–175 (2015) 225–243.
- [13] R.J. van Putten, J.C. van der Waal, E. de Jong, C.B. Rasrendra, H.J. Heeres, J.G. de Vries, *Chem. Rev.* 113 (2013) 1499–1597.
- [14] H.-Y. Wang, H. Qian, W.R. Yao, *Food Chem.* 128 (2011) 573–584.
- [15] K.W. Omari, J.E. Besaw, F.M. Kerton, *Green Chem.* 14 (2012) 1480–1487.
- [16] Y. Ohmi, S. Nishimura, K. Ebitani, *ChemSusChem* 6 (2013) 2259–2262.
- [17] Y. Hrynets, M. Ndagiijimana, M. Betti, *J. Agric. Food Chem.* 63 (2015) 6249–6261.
- [18] S. Wu, H. Fan, Q. Zhang, Y. Cheng, Q. Wang, G. Yang, B. Han, *Clean-Soil Air Water* 39 (2011) 572–576.
- [19] H. Tsuchida, M. Komoto, H. Kato, M. Fujimaki, *Agric. Biol. Chem.* 37 (1973) 2571–2578.
- [20] J. Rohovec, J. Kotek, J.A. Peters, T. Maschmeyer, *Eur. J. Org. Chem.* (2001) 3899–3901.
- [21] K. Sumoto, M. Irie, N. Mibu, S. Miyano, Y. Nakashima, K. Watanabe, T. Yamaguchi, *Chem. Pharm. Bull.* 39 (1991) 792–794.
- [22] A.P. Zhu, J.B. Huang, A. Clark, R. Romero, H.R. Petty, *Carbohydr. Res.* 342 (2007) 2745–2749.
- [23] M.C. Agyei-Aye, J.H. Lauterbach, S.C. Moldoveanu, *Carbohydr. Res.* 337 (2002) 2273–2277.
- [24] L. Jia, Y. Wang, Y. Qiao, Y. Qi, X. Hou, *RSC Adv.* 4 (2014) 44253–44260.
- [25] Detailed information on reagent price can be found at: <http://www.scbt.com/zh/datasheet-211545-fructosazine.html> <http://www.scbt.com/zh/datasheet-206528-2-5-deoxyfructosazine.html>.
- [26] N. Kashige, T. Yamaguchi, N. Mishiro, H. Hanazono, F. Miake, K. Watanabe, *Biol. Pharm. Bull.* 18 (1995) 653–658.
- [27] C.M. Gordon, *Appl. Catal. A: Gen.* 222 (2001) 101–117.
- [28] M.T. Clough, K. Geyer, P.A. Hunt, S. Son, U. Vagt, T. Welton, *Green Chem.* 17 (2015) 231–243.
- [29] X. Chen, B. Souvanthong, H. Wang, H. Zheng, X. Wang, M. Huo, *Appl. Catal. B: Environ.* 138–139 (2013) 161–166.
- [30] K. Yan, Y. Yang, J. Chai, Y. Lu, *Appl. Catal. B: Environ.* 179 (2015) 292–304.
- [31] E.A. Khokhlova, V.V. Kachala, V.P. Ananikov, *ChemSusChem* 5 (2012) 783–789.
- [32] P. Carniti, A. Gervasini, F. Bossola, V.D. Santo, *Appl. Catal. B: Environ.* 193 (2016) 93–102.
- [33] M.J. Frisch, G.W. Trucks, H.B. Schlegel, G.E. Scuseria, M.A. Robb, J.R. Cheeseman, G. Scalmani, V. Barone, B. Mennucci, G.A. Petersson, H. Nakatsuji, M. Caricato, X. Li, H.P. Hratchian, A.F. Izmaylov, J. Bloino, G. Zheng, J.L. Sonnenberg, M. Hada, M. Ehara, K. Toyota, R. Fukuda, J. Hasegawa, M. Ishida, T. Nakajima, Y. Honda, O. Kitao, H. Nakai, T. Vreven, J.A. Montgomery Jr., J.E. Peralta, F. Ogliaro, M. Bearpark, J.J. Heyd, E. Brothers, K.N. Kudin, V.N. Staroverov, R. Kobayashi, J. Normand, K. Raghavachari, A. Rendell, J.C. Burant, S.S. Iyengar, J. Tomasi, M. Cossi, N. Rega, N.J. Millam, M. Klene, J.E. Knox, J.B. Cross, V. Bakken, C. Adamo, J. Jaramillo, R. Gomperts, R.E. Stratmann, O. Yazyev, A.J. Austin, R. Cammi, C. Pomelli, J.W. Ochterski, R.L. Martin, K. Morokuma, V.G. Zakrzewski, G.A. Voth, P. Salvador, J.J. Dannenberg, S. Dapprich, A.D. Daniels, O. Farkas, J.B. Foresman, J.V. Ortiz, J. Cioslowski, D.J. Fox, Gaussian 09 Revision D. 01, Gaussian, Inc, Wallingford, CT, 2013.
- [34] M.L. Kuznetsov, B.G.M. Rocha, A.J.L. Pombeiro, G.B. Shul'pin, *ACS Catal.* 5 (2015) 3823–3835.
- [35] D. Sheberla, B. Tumanskii, A.C. Tomasik, A. Mitra, N.J. Hill, R. West, Y. Apeloig, *Chem. Sci.* 1 (2010) 234–241.
- [36] A.D. Becke, *J. Chem. Phys.* 98 (1993) 5648–5652.
- [37] C. Lee, W. Yang, R.G. Parr, *Phys. Rev. B* 37 (1988) 785–789.
- [38] G. Yang, E.A. Pidko, E.J.M. Hensen, *J. Catal.* 295 (2012) 122–132.
- [39] E.H.M. Elageed, B. Wang, Y. Zhang, S. Wu, G. Gao, *J. Mol. Catal. A: Chem.* 408 (2015) 271–277.
- [40] B. Wang, Z. Luo, E.H.M. Elageed, S. Wu, Y. Zhang, X. Wu, F. Xia, G. Zhang, G. Gao, *ChemCatChem* 6 (2014) 278–283.
- [41] J. Velasco, E. Perez-Mayoral, V. Calvino-Casilda, A.J. Lopez-Peinado, M.A. Banares, E. Soriano, *J. Phys. Chem. B* 119 (2015) 12042–12049.
- [42] P.J. Hay, *J. Chem. Phys.* 66 (1977) 4377–4384.
- [43] R. Krishnan, J.S. Binkley, R. Seeger, J.A. Pople, *J. Chem. Phys.* 72 (1980) 650–654.
- [44] A.D. McLean, G.S. Chandler, *J. Chem. Phys.* 72 (1980) 5639–5648.
- [45] A.J.H. Wachters, *J. Chem. Phys.* 52 (1970) 1033–1036.
- [46] Y. Takano, K.N. Houk, *J. Chem. Theory Comput.* 1 (2005) 70–77.
- [47] M. Cossi, N. Rega, G. Scalmani, V. Barone, *J. Comput. Chem.* 24 (2003) 669–681.
- [48] V. Barone, M. Cossi, *J. Phys. Chem. A* 102 (1998) 1995–2001.
- [49] S. Grimme, S. Ehrlich, L. Goerigk, *J. Comput. Chem.* 32 (2011) 1456–1465.
- [50] M. Swart, M. Sola, F.M. Bickelhaupt, *J. Comput. Chem.* 32 (2011) 1117–1127.
- [51] L. Goerigk, S. Grimme, *Phys. Chem. Chem. Phys.* 13 (2011) 6670–6688.
- [52] S. Wang, X. Guo, T. Liang, Y. Zhou, Z. Luo, *Bioresour. Technol.* 104 (2012) 722–728.
- [53] X. Huang, D.G. Cheng, F. Chen, X. Zhan, *Bioresour. Technol.* 143 (2013) 447–454.
- [54] H. Zhang, J. Liu, J. Shen, X. Jiang, *Energy* 82 (2015) 312–321.
- [55] B.R. Brooks, C.L. 3rd, Brooks, A.D. Mackerell Jr., L. Nilsson, R.J. Petrella, B. Roux, Y. Won, G. Archontis, C. Bartels, S. Boresch, A. Cafisch, L. Caves, Q. Cui, A.R. Dinner, M. Feig, S. Fischer, J. Gao, M. Hodosek, W. Im, K. Kuczera, T. Lazaridis, J. Ma, V. Ovchinnikov, E. Paci, R.W. Pastor, C.B. Post, J.Z. Pu, M. Schaefer, B. Tidor, R.M. Venable, H.L. Woodcock, X. Wu, W. Yang, D.M. York, M. Karplus, *J. Comput. Chem.* 30 (2009) 1545–1614.
- [56] B.R. Brooks, R.E. Bruccoleri, B.D. Olafson, D.J. States, S. Swaminathan, M. Karplus, *J. Comput. Chem.* 4 (1983) 187–217.
- [57] K. Vanommeslaeghe, E. Hatcher, C. Acharya, S. Kundu, S. Zhong, J. Shim, E. Darian, O. Guvench, P. Lopes, I. Vorobiov, A.D. Mackerell Jr., *J. Comput. Chem.* 31 (2010) 671–690.
- [58] L. Martinez, R. Andrade, E.G. Birgin, J.M. Martinez, *J. Comput. Chem.* 30 (2009) 2157–2164.
- [59] X. Sun, Q. Tian, Z. Xue, Y. Zhang, T. Mu, *RSC Adv.* 4 (2014) 30282–30291.
- [60] D. Horton, J.S. Jewell, K.D. Philips, *J. Org. Chem.* 31 (1966) 4022–4025.
- [61] K.H. Gardner, L.E. Kay, *Annu. Rev. Biophys. Biomol. Struct.* 27 (1998) 357–406.
- [62] P. Vujićić, Z. Meić, D. Vikić-Topić, *Spectrosc. Lett.* 28 (2006) 395–405.
- [63] S. Siankevich, Z. Fei, R. Scopelliti, G. Laurenczy, S. Katsyuba, N. Yan, P.J. Dyson, *ChemSusChem* 7 (2014) 1647–1654.
- [64] J. Zhang, E. Weitz, *ACS Catal.* 2 (2012) 1211–1218.
- [65] R.S. Assary, P.C. Redfern, J. Greeley, L.A. Curtiss, *J. Phys. Chem. B* 115 (2011) 4341–4349.
- [66] M.R. Nimlos, S.J. Blanksby, G.B. Ellison, R.J. Evans, *J. Anal. Appl. Pyrolysis* 66 (2003) 3–27.
- [67] M.B. Steven, *J. Org. Chem.* 58 (1993) 5414–5421.
- [68] R.S. Assary, L.A. Curtiss, *Energy Fuels* 26 (2012) 1344–1352.
- [69] L. Yang, G. Tsilomelekis, S. Caratzoulas, D.G. Vlachos, *ChemSusChem* 8 (2015) 1334–1341.
- [70] R.S. Assary, T. Kim, J.J. Low, J. Greeley, L.A. Curtiss, *Phys. Chem. Chem. Phys.* 14 (2012) 16603–16611.
- [71] A.K. Chakraborti, S.R. Roy, *J. Am. Chem. Soc.* 131 (2009) 6902–6903.
- [72] T.G.A. Youngs, J.D. Holbrey, C.L. Mullan, S.E. Norman, M.C. Lagunas, C. D'Agostino, M.D. Mantle, L.F. Gladden, D.T. Bowron, C. Hardacre, *Chem. Sci.* 2 (2011) 1594–1605.
- [73] R.J. Rico, M. Page, C.D. Jr, *J. Am. Chem. Soc.* 114 (1992) 1131–1136.
- [74] D.C. Tardy, A.S. Gordon, W.P. Norris, *J. Phys. Chem.* 80 (1976) 1398–1400.
- [75] T. Akiyama, Y. Enomoto, T. Shibamoto, *J. Agric. Food Chem.* 26 (1978) 1176–1179.
- [76] S. Hu, Z. Zhang, J. Song, Y. Zhou, B. Han, *Green Chem.* 11 (2009) 1746–1749.